Environ Earth Sci (2012) 67:1045–1060
DOI 10.1007/s12665-012-1564-8

ORIGINAL ARTICLE

A hydrochemical study of Hungtsaiping landslide area, Nantou, Taiwan

Pei-Ying Lin · Louis Loung-Yie Tsai

Received: 7 July 2010 / Accepted: 12 January 2012 / Published online: 7 February 2012

Abstract The Hungtsaiping landslide was triggered by the Chi-Chi earthquake (Mw = 7.6), which occurred on September 20, 1999 near the town of Chi-Chi in Nantou County in central Taiwan. The purpose of this study is to understand the relationship between geochemical characteristics and the landslide in the Hungtsaiping area. Water samples were collected from springs, creeks, ponds, groundwater and the Yonglu stream once every month from May 2008 to May 2009. Oxygen and hydrogen stable isotopes, ionic concentrations, electrical conductivities, and pH values were analyzed. The results show that the ionic concentrations display a significant spatial variation. For instance, calcium and magnesium bicarbonate-rich water was found on the top and the middle part of the slope. In addition, sodium bicarbonate-rich water with exceptionally high sulfate concentration was found on the foot of the slope. The sulfate content decreased with increasing elevation along the slope. Finally, a conceptual model was established by summarizing the hydrogeochemical analyses. After a scientific understanding of the mechanism of the Hungtsaiping landslide, all of the analytical information can be integrated for hazard prevention in the future.

Keywords Landslide · Geochemical characteristics · Oxygen and hydrogen isotope · Hydrochemistry

P.-Y. Lin · L. L.-Y. Tsai (✉)
Institute of Applied Geology, National Central University, Taoyuan County 320, Zhongli, Taiwan
e-mail: ltsai@app.geo.ncu.edu.tw

Introduction

Taiwan is part of an active mountain belt created by the oblique collision between the Philippine Sea Plate and Eurasian Plate. A complex geological structure and steep topography were thus developed. Furthermore, the severe climate, particularly increased frequency and intensity of rainfall due to typhoon events, was another factor that may induce landslides. In addition, the increasing population and economic development in Taiwan raised more risks associated with the landslide and debris flow. Hence, field investigation and monitoring work to prevent, mitigate, and provide early warning become more and more important. In the past, the methods of landslide research included interpretation of aerial photos and topographic maps, field investigation, geophysical exploration, borehole logging, laboratory experiments and on-site monitoring of parameters such as the depth of water table (Peng et al. 2008; Liu et al. 2008). Chen et al. (2005) suggested that mass loading and slope gradient are two major factors affecting slope stability in a slide-prone area. Water also plays an important role for mass movement in a slope region (Peng et al. 2007). Although hydrological triggering can be considered to be the most common mechanism of initiation and reactivation of landslides, water flows inside the system that involve the source and pathway of the waters have also been shown to have a major impact (de Montety et al. 2007; Guglielmi et al. 2002). Since the 1990s, many studies have concerned the characteristics of hydrochemistry, because hydrogeochemical information can unravel the hydrological processes that trigger landslides (Bogaard et al. 2007). Hydrogeochemistry is considered an effective tool for landslide study. Thus, over the past few decades, the focus of landslide research has shifted from emphasizing the variation of morphology to the hydrogeochemical characteristics.

Hydrochemistry displays a significant spatial and temporal variation. The hydrochemical analysis not only has the advantage of defining the boundary conditions of the landslide complexes (de Montety et al. 2007), but can lead directly to the determination of the different zones in a drainage system (Guglielmi et al. 2000). Hydrochemical evolution can be readily explained by combining geochemical processes, such as dilution, dissolution-precipitation of carbonate minerals, cation exchange, and pyrite dissolution (Bogaard et al. 2007). For example, the chemical dilution at spring waters can be correlated with precipitation, infiltration period, transit time, and the rate of landslide movement (Cappa et al. 2004; de Montety et al. 2007). The most important concept is that hydrochemical information can be used to determine the origin and pathway of water (Wang et al. 2001) and display the short- and long-term hydrological evolution of landslide materials. Therefore, the objectives of this study are as follows: (a) to use hydrogeochemical information to unravel the hydrological processes in triggering landslides; (b) to develop a conceptual model of hydrological flow processes and water origin in the Hungtsaiping landslide; and (c) to comprehend the relation between geochemical characteristics and the mechanism of landslide.

Study area

Hungtsaiping is located on the south bank of the Yonglu stream (the upper branch of the Jhangping Stream) in the Chungliao village of Nantou County in central Taiwan. On September 20, 1999 at 17:47 UTC, an earthquake of magnitude 7.6 occurred near the town of Chi-Chi in Nantou County in central western Taiwan. The epicenter was located at 23.77°N, 120.98°E, approximately 8.0 km in focal depth. The Chi-Chi earthquake was the largest magnitude earthquake ever recorded in Taiwan in the twentieth century. Past experience in Taiwan has shown that the most noteworthy damage after the earthquake is a landslide. The size of earthquake-induced landslides depend on several essential factors, such as the magnitude and the focal depth of the earthquake, the topography and geologic conditions near the fault, as well as the frequency and duration of ground shaking (Hays 1981). Thousands of landslides triggered by the Chi-Chi earthquake include gully-type debris flows at the 99 Peaks (Liu et al. 2008), gigantic and deep-seated slides of Taoling and Jiufengershan (Wang et al. 2003), and a large landslide at Hungtsaiping (Wei and Lee 2006). Landslides include various types of shallow- or deep-seated movements; moreover, the regional geological and geomorphological characteristics can be used as the control factors of landslides. Geologically, Hungtsaiping landslide is located at the west side of Tsukeng Anticline, other geological structures nearby the Hungtsaiping area include Tahengpingshan Syncline, Shuilikeng Fault, Dingshuiku Fault, Kweipu Fault, and Shuangtung Fault, as shown in Fig. 1. Moreover, outcropped formations in the area include Tanliaoti Shale (Tl), Shihmen Formation (Sm), Changhukeng Shale (Ch), and Shenkeng Sandstone (Sk), all belong to Miocene in age. The detailed features are summarized in Table 1 (Huang et al. 2000). The covered colluvium in the Hungtsaiping area can be divided into three parts: rock, colluvium and interlayer. The borehole logging information is listed in Table 2. The drilled core of regional stratum is mostly composed of shale and colluvium, except BH-9 and BH-10, which include 32-m-thick sandstones. Since the interface of batholith and shale was found near the sampling locations of the Yonglu stream-3 and 4, it is conjectured that the Yonglu stream is the boundary of the Hungtsaiping landslide. The Hungtsaiping area belongs to the Wu-chi basin and has an annual mean temperature of 24.2°C. According to the Central Weather Bureau, the mean monthly maximum temperature is 27.3°C in July, and the mean monthly minimum temperature is 19.5°C in January. Moreover, the annual accumulated precipitation is 2,144.71 mm, with rainfall concentrated from May to September. Most of the landslides are genetically related to plum rain, typhoons, and topography. After typhoons, many small-scale and shallow landslides may take place. For instance, Kalmaegi (2008/07/16–18) and Fung-Wong (2008/07/26–29) induced a landslide near BH-12 on the Yonglu stream-3 and 4, and Sinlaku (2008/09/11–16) induced a landslide near A GullyEast-1and Out 1–3.

Sampling and analytical methods

Water sampling was conducted from May 2008 to May 2009. 19 groundwater samples were collected from the boreholes that were drilled in 2005 and 2008. In addition, 15–18 surface water samples were collected monthly from creeks, ponds, spring waters and the Yonglu stream. Electrical conductivity and pH were measured in the laboratory. Moreover, specific ion concentrations (Cu^{2+}, Fe^{2+}, Mg^{2+}, Ca^{2+}, Na^{+}, K^{+}, SO_4^{2-}, and Cl^{-}) were determined by atomic absorption spectrometry (AA) and high-pressure ionic chromatography (IC). The bicarbonate concentration was determined by titration. The total relative uncertainty, including the device accuracy and the repeatability error, was less than 5%. Nevertheless, for samples with unexpectedly high ionic concentration, a dilution up to a factor of 10–20 times was needed. The mean total uncertainty due to this dilution procedure was estimated to be 10–15% for the dominant species (Na^{+},

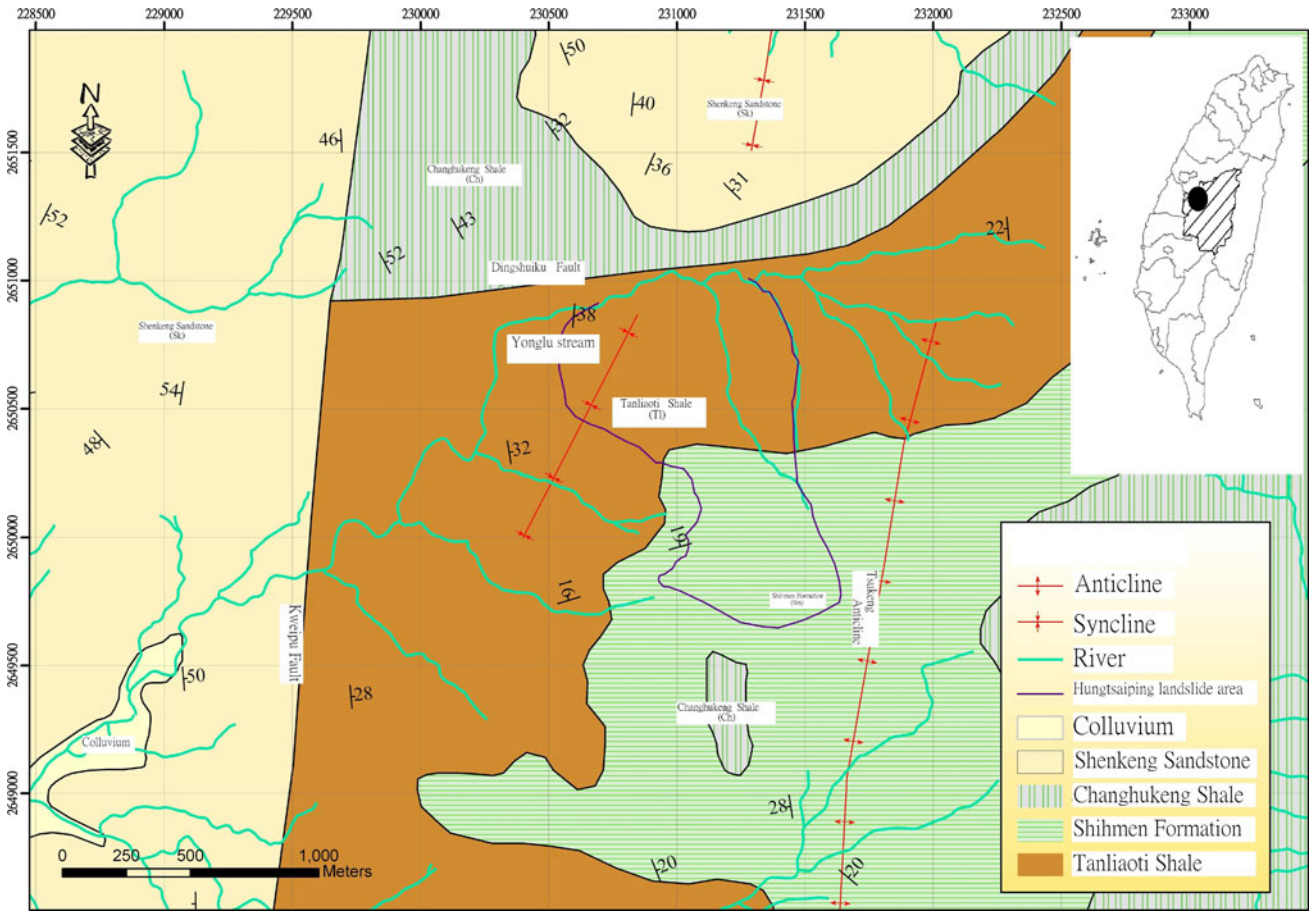

Fig. 1 The Geological map of Hungtsaiping area with main structural features

Mg^{2+}, Ca^{2+}, SO_4^{2-}, Cl^-) and less than 10% for other compounds.

The isotopic composition of oxygen was analyzed by the CO_2–H_2O equilibration method, using a VG SIRA 10 isotope ratio mass spectrometer (Epstein and Mayeda 1953), and the hydrogen isotopic composition was determined on a VG MM602D isotope ratio mass spectrometer (IRMS) after reduction of water to H_2 by using zinc (Coleman et al. 1982). The laboratory standards of analytical precisions were ±0.1‰ for $\delta^{18}O$ and ±1.5‰ for δD.

Results and discussion

Classification of water samples

Water samples can be classified and categorized. First, samples were divided into surface water and groundwater according to their sampling locations. Second, surface water and groundwater were further grouped according to their water sources, the variation of water table, and borehole logging data (Table 3). The following discussion is based on this classification.

Hydrochemical characteristics

Knowledge of the hydrochemistry can be utilized to interpret the geochemical processes in a specific region. Water flows within the soil matrix by infiltrating the crack networks. If the crack network is only weakly linked, the chemical variation and groundwater level (Table 4) show similar trends all year round. This study is focused on the differences in the crack system. The hydrologic factors including intense infiltration, fast recharge rates, and excess dilution affect the development of the crack system in this region. The results of the descriptive statistical analysis revealed that each hydrochemistry parameter varies with group and space (Table 5). Each group of samples displays similar variation. For example, the largest variation in the monthly mean was in the ponds group, whereas the monthly mean of the creek group varied the least. In addition, water chemical characteristics were consistently related to topographical features (Fig. 2a–c).

Table 1 Stratigraphy of Hungtasiping area (revised from Huang et al. 2000)

	Stratigraphy	Thinkness (m)	Major description	
Miocene	Shenkeng sandstone (Sk)	450	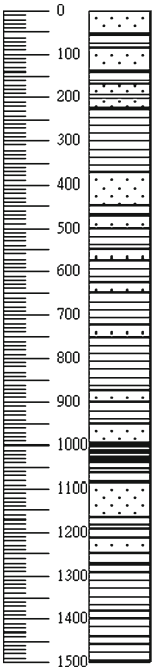	Thick, chunk sandstone and dark-gray shale which interlayered with thin sandstone. The middle of this formation has a lot fossils.
	Changhukeng shale (Ch)	500		Dark-gray, thick shale which intercalated with thin sandstone, and the shale is thick or chunk. It is any amount of glauconite, fossils such as foraminifera.
	Shihmen formation (Sm)	300		Dark-gray shale and three layers light-gray, fine to medium-grained, thick sandstone, rich in fossils such as shellfish except crustaceans and foraminifera.
	Tanliaoti shale (Tl)	250		Gray, thick shale layers intercalated with thin, fine-grained sandstone, great quantity of glauconite, fossils such as marine foraminifer, shellfish except crustaceans and so forth.

Table 2 Characteristics of the boreholes

ID	Coordinates		Height (m)	Depth (m)	Thickness of colluvial layer (m)
	X	*Y*			
BH-2	231289	2650759	591.0	84.0	82.35
BH-3	231354	2650816	590.0	67.0	63.20
BH-4	231339	2650840	588.0	78.5	68.40
BH-6	231444	2650252	712.0	19.0	13.20
BH-7	231408	2650264	709.0	30.0	27.00
BH-9	230906	2650594	595.0	128.0	76.85
BH-10	230814	2650459	584.0	71.0	37.35
BH-12	230769	2650748	520.0	40.0	6.50
EH-1	230855	2650737	532.0	50.0	24.45
EH-5	230828	2650789	512.0	80.0	19.77
EH-9	230896	2650803	522.0	10.0	>10.00
EH-11	230815	2650825	502.0	50.0	17.00

Moreover, the variations of monthly mean data in the hydrogeochemistry measurements from the deep aquifers were larger than those from the shallow aquifer. These findings can be explained by geochemical processes; the distribution of the water chemistry also provides insight into the continuity of the groundwater system (Fig. 2d–f). The trends were characterized by both high sulfate and high calcium concentrations in the creek group (SO_4^{2-} up to 160.79 ppm; Ca^{2+} up to 73.64 ppm, data recorded in May 2008 and April 2009, respectively) and the spring water group (SO_4^{2-} up to 126.78 ppm; Ca^{2+} up to 74.92 ppm, both recorded in April 2009). However, the

Table 3 Classification of the water samples

Groups	Sampling locations		
Surface water			
Ponds	Moon Peach Lake		
	A Shao Shui Ku		
	Out 3-Shao Shui Ku		
Creeks	Out 2-Moon Peach Alley Bridge		
	A Gully-top		
	A Gully-bottom		
	AB Gully-down		
	AB Gully-bottom		
	C upper creek		
	The Yonglu stream-1		
	The Yonglu stream-4		
Springs	A Gully East-1		
	A Gully East-2		
	A Gully East-3		
	A Gully East-4		
	A Gully East-5		
	Out 1		
	The Yonglu stream-2 (seepages)		
	The Yonglu stream-3 (seepages)		
	The Yonglu stream-5 (seepages)		
	The Yonglu stream-6 (seepages)		
	The Yonglu stream-7 (seepages)		
Groundwater			
Shallow aquifers	BH-2(A)	BH-2(B)	BH-7(A)
	BH-7(B)	BH-9(B)	BH-10(B)
	BH-12(B)	EH-09	EH-11(B)
Deep aquifers	BH-3(A)	BH-3(B)	BH-9(A)
	BH-10(A)	BH-12(A)	EH-01
	EH-11(A)		

trends of the pond group were different from others. The unexpectedly high concentrations of SO_4^{2-}, Mg^{2+} and Na^{+} could be explained as the contribution of deep water moving along major discontinuities, such as faults, bedding and schistosity planes. A more detailed understanding of the results can be gained by examining the origin and pathway of surface water. Meteoric water was the major recharge source, and the chemical features varied after rain events. Consequently, the sources of creeks and spring waters were identical and differ from those of ponds. Moreover, the ponds had an additional recharge during April to May 2009.

Thermodynamic calculations demonstrated that the water had a higher sulfate concentration when it drained through a longer distance and spent greater time inside the slope region. In fact, all of the signals during the precipitation periods illustrated the influence of geochemical reactions, which included dilution, chemical precipitation, infiltration, and the mixing of meteoric water with groundwater. In brief, water will reactivate chemically near the equilibrium state between the reservoir and the rock. The geochemical reactions were characterized by high concentrations of ions in the deep aquifer (SO_4^{2-} up to 41.71 ppm; Ca^{2+} up to 72.27 ppm, data recorded in May 2009 and April 2009, respectively; Fig. 3a). The variation of hydrochemistry and precipitation in the Hungtsaiping landslide area appeared to be highly related among electrical conductivity, concentrations of Mg^{2+}, Ca^{2+}, Na^{+}, SO_4^{2-}, Cl^{-} and accumulated precipitation.

In all groups of water, the variations of ionic concentration decreased with increasing precipitation from June to July 2008 and August to September 2008 can be attributed to dilution. There was no precipitation from October 2008 to February 2009. During that time, the concentrations of most species displayed steady and the least variation in the shallow aquifer. In conclusion, dilution caused by

Table 4 The classified catalogue of groundwater and the data of monthly variation of water table (unit: meter)

Geologic material	BH-2(A) I	BH-2(B) C	BH-3(A) I	BH-3(B) C	BH-7(A) I	BH-7(B) C	BH-9(A) R	BH-9(B) C	BH-10(A) R	BH-10(B) I	BH-12(A) R	BH-12(B) I	EH-01 R	EH-09 I	EH-11(A) R	EH-11(B) I
May-08	576.45	584.35	564.32	568.34	707.80	705.25	553.31	583.38	539.75	571.02	499.85	518.51	–	–	–	–
Jun-08	–	584.44	564.42	568.43	–	–	554.52	585.56	545.13	571.41	500.96	519.26	–	–	–	–
Jul-08	576.47	584.56	564.32	568.23	–	706.65	553.88	586.61	546.88	572.27	501.06	519.16	–	–	–	–
Aug-08	576.59	584.23	–	568.29	710.45	707.05	–	585.65	–	572.53	501.23	518.91	–	–	–	–
Sep-08	576.51	584.68	564.43	568.29	709.84	707.17	554.91	587.30	548.68	572.76	501.43	519.30	520.42	524.29	489.90	499.56
Oct-08	576.38	584.86	564.46	568.28	709.15	706.80	555.63	585.11	545.43	573.22	502.41	518.88	508.94	523.33	488.04	494.86
Nov-08	576.27	584.82	564.40	568.27	707.13	705.38	555.68	584.00	542.67	573.08	501.90	518.49	507.67	522.92	483.90	490.93
Dec-08	576.94	584.80	564.60	568.45	706.55	705.32	556.14	584.12	542.02	572.84	504.76	515.46	506.45	522.86	483.90	489.04
Jan-09	576.21	584.29	564.28	568.10	705.95	704.94	554.94	583.37	541.12	572.23	500.94	514.57	505.31	522.79	483.91	486.48
Feb-09	576.12	584.21	564.27	568.09	705.57	704.71	553.74	583.31	540.57	571.64	499.61	514.61	504.65	522.71	483.89	485.78
Mar-09	576.20	584.46	564.59	568.88	706.11	705.21	552.28	584.96	540.77	571.18	500.33	516.61	504.40	522.68	483.93	486.16
Apr-09	576.36	584.22	–	–	705.24	705.19	552.16	584.78	540.32	571.16	499.97	518.69	504.30	522.75	483.95	486.38
May-09	576.26	584.31	564.62	569.03	707.59	706.44	552.53	586.48	542.65	571.44	499.64	516.73	504.27	522.94	483.92	486.41
Mean	576.40	584.48	564.43	568.39	707.40	705.84	554.14	584.97	543.00	572.06	501.08	517.63	507.38	523.03	485.04	489.51
Height of borehole	591.00	591.00	590.00	590.00	709.00	709.00	595.00	595.00	584.00	584.00	520.00	520.00	532.00	522.00	502.00	502.00
	S	S	D	D	S	S	D	S	D	S	D	S	D	S	D	S

R rock, *C* colluvial, *I* interface, *S* shallow aquifer, *D* deep aquifer

Table 5 Monthly mean data of groups: ponds, creeks, spring waters, deep aquifer and shallow aquifer from the fractured zone of landslide

	2008								2009				
	May	Jun	Jul	Aug	Sep	Oct	Nov	Dec	Jan	Feb	Mar	Apr	May
pH													
Ponds	8.19	8.12	8.17	7.95	8.02	8.37	8.27	8.37	8.37	7.32	7.11	7.28	7.18
Creeks	8.36	8.26	8.35	8.24	8.37	8.43	8.45	8.49	8.45	8.39	7.93	8.00	8.03
Springs	8.33	8.17	8.34	8.16	8.36	8.41	8.47	8.57	8.44	8.46	8.25	8.09	8.21
Deep aquifer	8.48	8.59	8.70	8.57	8.42	8.58	8.47	8.50	8.48	7.98	7.73	7.48	7.62
Shallow aquifer	8.34	8.42	8.60	8.42	8.28	8.37	8.30	8.40	8.32	7.97	7.92	7.73	7.85
EC (μS)													
Ponds	542.7	393.0	305.8	453.7	177.7	228.3	305.6	259.4	270.4	360.0	379.6	306.5	344.0
Creeks	646.4	445.4	337.4	424.1	311.4	354.8	421.5	426.7	512.0	661.9	670.6	637.9	539.7
Springs	568.9	440.7	328.7	382.9	290.0	307.7	382.7	436.0	496.6	653.9	715.6	680.4	636.4
Deep aquifer	825.5	822.5	686.1	786.1	537.8	555.4	546.6	628.1	676.1	741.5	812.7	796.6	752.4
Shallow aquifer	636.4	648.9	555.4	623.5	369.9	361.2	364.4	374.2	408.7	530.1	570.1	685.3	706.4
SO_4^{2-} (ppm)													
Ponds	141.44	59.22	45.70	84.52	24.42	17.56	59.59	30.89	28.85	27.90	28.82	30.15	119.37
Creeks	160.79	83.12	52.37	65.07	42.08	50.99	74.71	74.43	92.75	118.82	134.53	123.08	94.26
Springs	115.25	74.47	30.17	55.49	36.39	42.44	50.55	55.81	66.61	99.77	114.49	126.78	80.29
Deep aquifer	30.17	32.52	9.69	26.63	21.76	28.96	25.07	26.69	29.21	31.77	33.69	29.27	41.71
Shallow aquifer	20.49	26.60	8.82	22.52	23.53	22.85	22.28	23.49	24.36	26.21	24.04	26.62	33.73
Cl^- (ppm)													
Ponds	6.33	3.80	2.71	3.70	3.26	1.98	2.00	2.15	2.29	2.88	4.21	3.26	1.92
Creeks	4.09	2.98	2.50	2.66	2.48	2.55	3.02	3.16	3.59	3.90	3.78	3.31	1.89
Springs	3.25	2.86	2.08	3.03	2.32	2.39	2.84	2.86	2.81	3.63	3.31	3.01	1.68
Deep aquifer	19.34	14.85	7.56	12.83	10.02	9.99	9.99	14.24	14.89	20.74	16.53	17.47	10.93
Shallow aquifer	5.28	5.30	2.75	5.16	4.35	4.22	4.33	4.32	4.25	4.62	4.40	4.72	3.55
HCO_3^- (ppm)													
Ponds	186.67	211.11	180.00	160.00	148.33	133.33	128.33	143.33	148.33	208.33	193.33	143.33	155.00
Creeks	221.90	199.05	244.76	202.86	188.89	186.11	187.78	201.43	222.95	271.90	249.05	206.67	200.00
Springs	230.00	201.48	247.50	180.00	175.24	180.95	207.62	220.48	259.05	296.25	295.42	224.58	242.92
Deep aquifer	448.57	437.14	555.24	432.38	337.00	321.33	318.33	355.00	383.00	393.00	398.00	388.67	365.33
Shallow aquifer	455.24	364.76	470.48	406.67	249.63	224.81	218.15	217.04	242.96	302.50	294.81	362.96	367.41
Mg^{2+} (ppm)													
Ponds	38.87	16.87	10.37	19.79	7.87	11.48	15.56	12.79	13.32	14.43	12.91	11.31	20.32
Creeks	22.64	19.76	15.62	18.33	13.79	15.84	9.86	17.63	19.89	17.81	18.88	20.92	18.49
Springs	17.56	17.40	9.49	16.15	12.27	13.74	15.68	15.02	15.87	17.38	16.98	20.39	17.96
Deep aquifer	11.87	11.58	5.01	14.32	9.08	9.85	12.29	11.36	12.45	11.86	12.21	12.63	12.92
Shallow aquifer	7.88	8.70	4.69	9.14	7.20	7.58	10.64	9.44	9.00	9.77	9.91	10.82	11.68
Ca^{2+} (ppm)													
Ponds	48.18	39.24	28.41	44.78	24.73	30.18	41.02	33.18	35.46	38.20	35.93	30.56	40.14
Creeks	20.40	37.10	34.37	38.23	34.85	34.43	26.91	33.92	28.16	31.55	47.63	73.64	68.27
Springs	21.17	32.94	32.43	37.83	34.96	32.55	35.54	28.36	21.17	24.89	39.17	74.92	44.18
Deep aquifer	14.45	15.89	16.30	16.76	20.26	19.80	20.45	18.78	16.17	22.79	38.49	72.27	44.60
Shallow aquifer	15.59	17.91	18.97	16.70	24.87	21.10	23.61	24.44	21.24	32.58	48.81	89.11	49.29
Na^+ (ppm)													
Ponds	76.24	28.58	17.34	32.41	9.18	12.75	15.36	15.99	18.95	28.37	24.48	23.21	103.94
Creeks	168.79	47.70	33.97	43.77	32.57	41.51	57.43	113.41	110.28	144.41	101.53	114.84	45.14
Springs	118.52	38.31	16.37	41.44	23.88	41.74	61.37	90.35	110.62	169.33	138.96	85.25	47.79
Deep aquifer	262.48	233.64	96.02	220.59	157.14	159.41	156.34	201.94	214.21	226.11	209.05	224.93	288.72

Table 5 continued

	2008								2009				
	May	Jun	Jul	Aug	Sep	Oct	Nov	Dec	Jan	Feb	Mar	Apr	May
Shallow aquifer	222.79	199.70	59.45	166.69	83.69	79.41	79.36	88.98	88.15	154.97	101.11	147.44	214.69
K^+ (ppm)													
Ponds	2.61	1.39	0.20	1.12	0.50	0.00	0.00	0.00	0.00	0.68	5.01	3.29	2.83
Creeks	0.90	0.47	0.41	1.11	0.39	0.38	1.25	0.39	0.46	0.24	3.13	3.66	5.76
Springs	0.04	0.35	0.24	0.54	0.06	0.02	0.51	0.00	0.00	0.43	2.59	3.11	2.72
Deep aquifer	0.56	0.41	0.00	0.68	3.76	0.63	0.43	0.61	0.88	0.83	2.83	3.34	2.68
Shallow aquifer	1.18	0.65	0.39	0.54	4.86	1.17	0.37	1.19	1.36	1.17	3.39	6.19	6.27
Fe^{2+} (ppm)													
Ponds	0.08	0.06	0.03	0.25	0.01	0.00	0.23	0.00	0.13	0.00	0.05	0.16	0.44
Creeks	0.10	0.07	0.02	0.00	0.01	0.03	0.00	0.00	0.07	0.00	0.33	0.02	0.02
Springs	0.09	0.07	0.03	0.00	0.04	0.03	0.00	0.00	0.08	0.00	0.08	0.03	0.02
Deep aquifer	0.08	0.06	0.06	0.00	0.01	0.02	0.00	0.01	0.35	0.10	0.08	0.16	0.08
Shallow aquifer	0.05	0.04	0.03	0.00	0.00	0.07	0.05	0.02	0.16	0.00	0.53	0.11	0.05
Cu^{2+} (ppm)													
Ponds	0.00	0.00	0.00	0.01	0.01	0.01	0.00	0.01	0.01	0.00	0.01	0.01	0.01
Creeks	0.00	0.00	0.00	0.01	0.00	0.01	0.00	0.00	0.01	0.00	0.00	0.01	0.01
Springs	0.00	0.00	0.00	0.01	0.00	0.00	0.00	0.00	0.01	0.00	0.00	0.01	0.01
Deep aquifer	0.00	0.00	0.00	0.00	0.00	0.01	0.00	0.00	0.01	0.00	0.00	0.01	0.01
Shallow aquifer	0.00	0.00	0.00	0.00	0.00	0.00	0.00	0.00	0.01	0.00	0.00	0.01	0.01

precipitation in the shallow aquifer had an obvious effect in summer of 2009 (Fig. 3b). In addition, meteoric water stored in the mountain region will provide recharge and lead to variation in hydrochemical trends in the deep aquifer during the dry season. Similar to deep aquifer, there was a strong positive correlation between electrical conductivity and the ion concentration in ponds (Fig. 3c). Moreover, in all groups, the concentrations of Mg^{2+}, Ca^{2+}, Na^+, K^+, SO_4^{2-}, Cl^- decreased after precipitation events. When there was no precipitation, the concentrations of most species remained stable and the variation was low. Thus, precipitation plays a significant role in the circulation of surface water.

The concentrations of ions provided important information about groundwater circulation within the landslide area. Due to their slow dissolution kinetics, sulfate and magnesium could be effective indicators of groundwater in most of the water types from carbonate aquifers containing-Ca^{2+}/Mg^{2+}–HCO_3^- and Na^+–HCO_3^-. Otherwise, ferruginous- and/or cupriferous-minerals were weathered by the physical and chemical weathering of minerals. Clearly, oxidation–reduction reactions indicate that recharged water had positive effects on the concentrations of Fe^{2+} and Cu^{2+}. In summary, most of the data in the pond and shallow aquifer had experienced strong oxidation-reduction reactions as shown in Table 5.

Isotopic characteristics

The oxygen and hydrogen isotopic compositions can provide crucial information on climate conditions and hydrogeological processes in a specific area. Based on the isotopic composition of the meteoric water collected from the Hungtsaiping area and compared with the historical data of Peng et al. (2002), the local meteoric water line of the Hungtsaiping area could be established as $\delta D = 8.4 \times \delta^{18}O + 18.0$. Meteoric water is the origin of the water cycle. In Taiwan, rainwater is the most proportion of meteoric water. Correlation of $\delta^{18}O$ and δ^2H isotopes of meteoric water can be plotted as: Meteoric Water Line (MWL). If the database of precipitation is restricted at a particular region, the equation is called Local Meteoric Water Line (LMWL); thus, it can be taken as the isotope background in the study area. By means of LMWL and the isotope composition of surface water, groundwater, and other water bodies can be recognized.

The isotopic composition of the monthly mean and accumulated precipitation from May 2008 to May 2009 in the Hungtsaiping area yielded useful information about the effects of precipitation and typhoons (Fig. 4). Typhoons are potentially bringing in rain and moving heat its impact can be examined by studying Oxygen-18 isotope. When precipitation increased due to typhoons, the stable isotopic

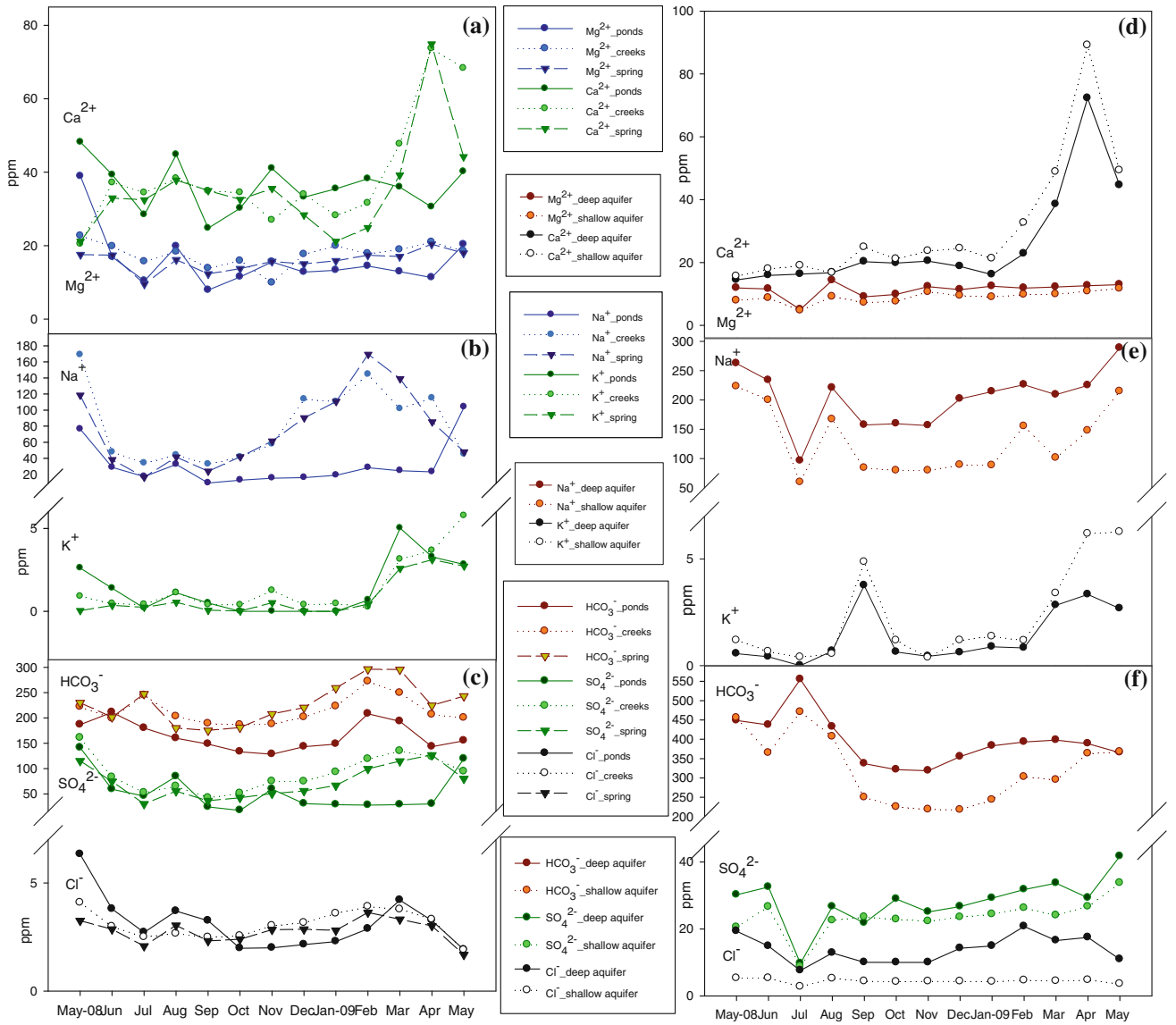

Fig. 2 Monthly mean concentrations in groups for surface water: **a** Mg^{2+} and Ca^{2+}; **b** Na^{+} and K^{+}; **c** HCO_3^{-} and SO_4^{2-} and Cl^{-} and groundwater; **d** Mg^{2+} and Ca^{2+}; **e** Na^{+} and K^{+}; **f** HCO_3^{-} and SO_4^{2-} and Cl^{-} during the study period in the Hungtsaiping area

composition became lighter conspicuously, and lasted for several months (Table 6). The findings indicated that precipitation had an effect on the isotopic composition in the Hungtsaiping area. The isotope compositions of water samples in the summer and/or high-elevation localities were lighter than in the winter and/or low elevation locations. The isotopic gradients can be used to deduce the recharge areas of spring water and infiltration. Several findings from $\delta^{18}O$ versus δD of samples were noticed. Although the variations of O and H isotope ratios between surface water and groundwater are not quite obvious, most of the stable isotopic compositions for groundwater were heavier than that of surface water, and the time-delay effect was common in groundwater. The time-delay effect displays transient variations after precipitation events, long-term hydrochemical variations, spatial distribution of the major cations and anions, the grade of mineralization, the pathway of infiltration and an aspect for the continuity of the groundwater system, the results can draw a conclusion on a conceptual model of flow processes and water origin in the specific landslide area.

For an extremely heavy rain in a short span of time such as typhoon and afternoon thundershower, the instant rainfall intensity will be extremely strong; there will be less infiltration, more surface runoff, and stronger erosion will occur. Simultaneously, if the drainage basin cannot drain the rainfall away quickly enough, surface erosion, and shallow landslides will become a serious problem. In addition, the water table will rise after continuous rain. When the water table reaches a certain level, the area will

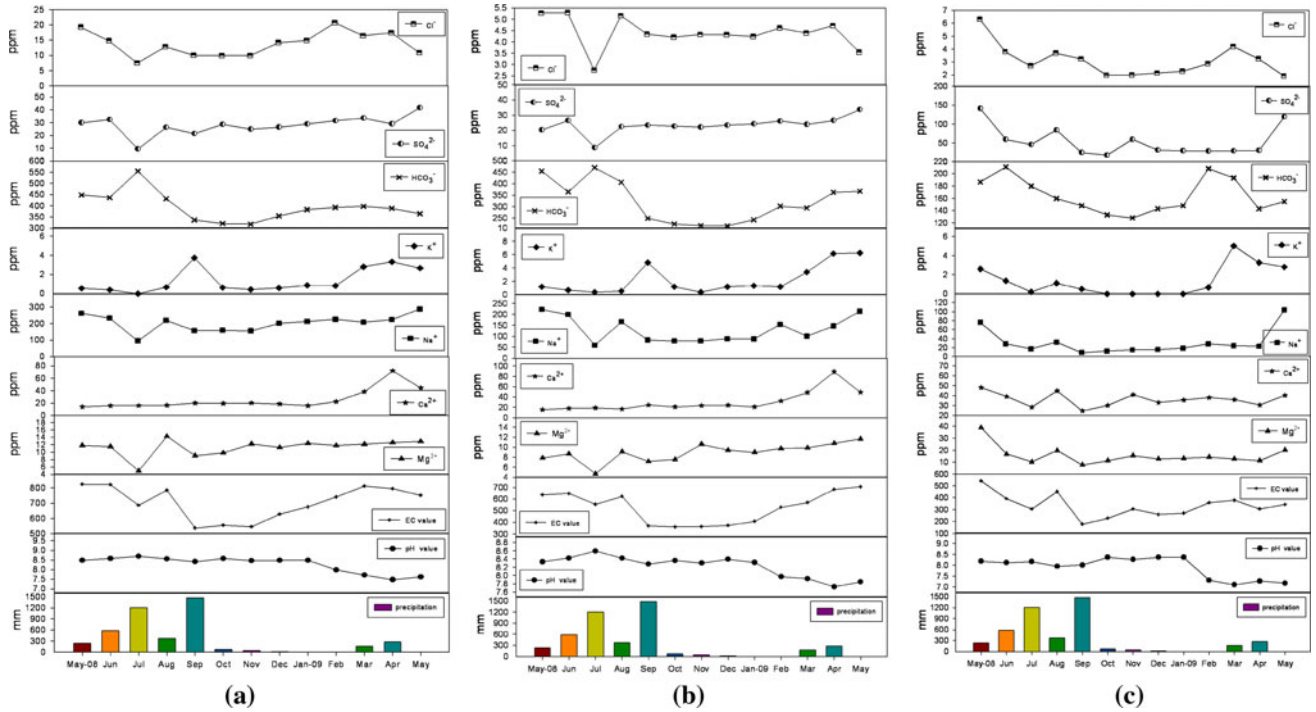

Fig. 3 Monthly mean measurements of groups **a** deep aquifer, **b** shallow aquifer, **c** ponds and precipitation during the study period in the Hungtsaiping area

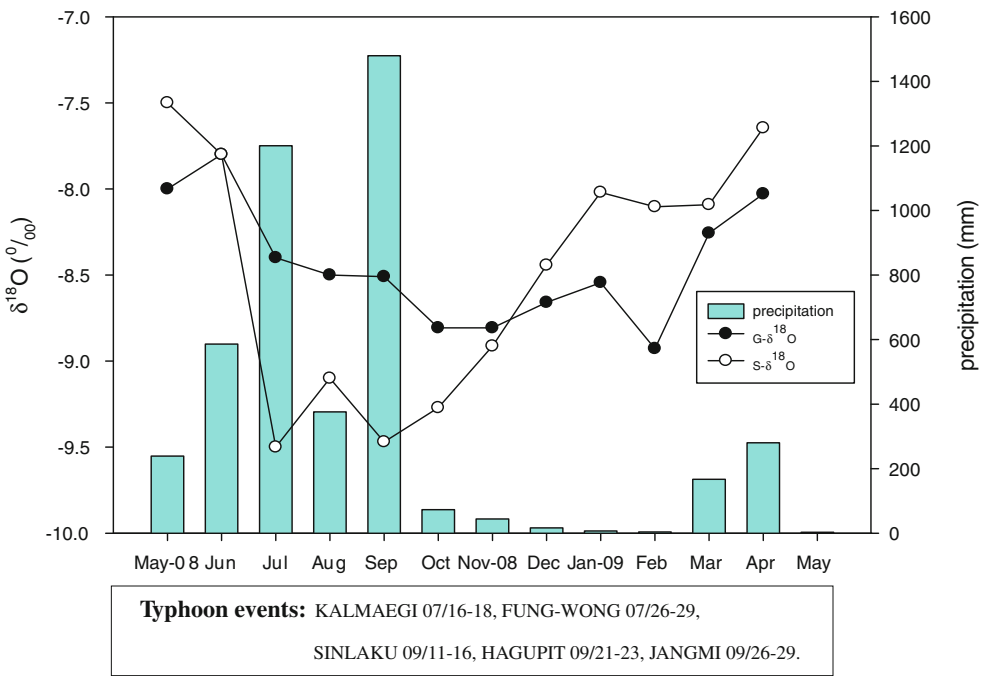

Fig. 4 Monthly isotopic compositions and precipitation from May 2008 to May 2009 in the Hungtsaiping area (*S* surface water, *G* groundwater)

possibly produce large-scale and deep-seated landslides on slopes, such as those that commonly occur during typhoon season. Thus, water is a crucial factor in landslide research. The compositions of hydrogen and oxygen isotopes were generally affected by altitude, precipitation, temperature, topography, season and evaporation, etc. Factors affecting the isotopes composition are discussed as follows: the altitude effect can lead to the decrease in $\delta^{18}O$ and $\delta^{2}H$ of precipitation at high elevation (Bogaard et al. 2007); the variation also depends on the local weather, temperature,

Table 6 Monthly mean isotopic compositions of water samples during studying periods in Hungtsaiping area: (a) ponds, (b) creeks, (c) spring waters, (d) deep aquifer and (e) shallow aquifer from the fractured zone of landslide

	(a) δ^{18}O (‰)	δD (‰)	d	(b) δ^{18}O (‰)	δD(‰)	d	(c) δ^{18}O (‰)	δD (‰)	d	(d) δ^{18}O (‰)	δD (‰)	d	(e) δ^{18}O (‰)	δD (‰)	d
May, 08	−5.7	−41	5.2	−7.8	−55	7.5	−7.9	−56	7.2	−7.8	−53	9.0	−8.3	−56	10.7
Jun, 08	−7.2	−52	5.6	−8.0	−56	8.1	−7.9	−55	8.4	−7.7	−54	7.7	−7.9	−56	7.0
Jul, 08*	−9.9	−71	8.3	−9.6	−67	9.9	−9.3	−65	10.1	−8.5	−58	10.7	−8.3	−56	9.7
Aug, 08	−9.0	−63	9.4	−9.2	−62	11.0	−9.1	−64	8.7	−8.3	−57	9.8	−8.8	−59	11.3
Sep, 08*	−9.3	−63	11.4	−9.5	−63	13.3	−9.5	−65	10.4	−8.6	−59	10.1	−8.4	−59	8.4
Oct, 08	−8.8	−62	8.1	−9.4	−63	12.4	−9.3	−63	12.0	−8.9	−62	9.7	−8.7	−60	9.3
Nov, 08	−8.5	−59	8.9	−8.7	−62	7.3	−9.2	−63	10.4	−8.8	−61	9.6	−8.4	−58	8.9
Dec, 08	−8.7	−59	11.2	−8.3	−56	10.8	−8.5	−57	11.1	−8.8	−60	10.0	−8.5	−58	10.2
Jan, 09	−8.0	−51	12.2	−7.7	−50	11.1	−8.4	−54	13.0	−8.7	−57	12.6	−8.4	−55	12.9
Feb, 09	−8.3	−56	9.9	−7.9	−51	11.9	−8.3	−54	12.5	−8.8	−56	13.9	−9.1	−58	15.3
Mar, 09	−7.7	−50	11.3	−8.1	−54	10.8	−8.2	−54	11.7	−8.4	−56	11.2	−8.1	−54	11.3
Apr, 09	−7.5	−50	9.9	−7.4	−48	11.4	−8.0	−50	13.0	−8.1	−54	10.7	−7.9	−52	11.6
May, 09	−8.9	−59	12.6	−8.5	−55	12.3	−9.3	−59	13.4	−8.6	−56	13.5	−8.0	−51	13.0

* The number of typhoon events

and topography. In light of the relationship between isotopes composition and altitude, δ^{18}O composition can be used to interpret the origin and flow paths of water within a slope region (Peng et al. 2007; Guglielmi et al. 2002). These environmental conditions have a great effect upon isotope fractionation. Furthermore, the isotope composition can reveal the water behaviors and the movement in different water bodies, and the data can further provide evidences of water evolution in the hydrosphere.

Precipitation is another important factor in isotope studies. During a precipitation event, meteoric water with a heavier isotope composition (δ^{18}O: −3.7‰; δD: −27‰ on 2008/11/08) fell, earlier than that with a lighter isotope composition (δ^{18}O: −7.6‰; δD: −55‰ on 2008/11/09. Consequently, the isotope composition is relatively lighter in strong precipitation (δ^{18}O: −6.9‰; δD: −47‰ on 2009/04/22) than in a small shower (δ^{18}O: −4.9‰; δD: −22‰ on 2009/02/20). In other words, as precipitation becomes heavier, the δ^{18}O composition becomes lighter. A similar seasonal effect has been observed in Taiwan. In the warm southwest monsoon season (May–October), the isotope composition of precipitation was relatively lighter compared to the cool northeast monsoon season (November–April). The oxygen isotope composition of all groups became lighter due to precipitation events from May to October 2008, but the groups began to differ after November 2008. This finding can be explained as there was no extra recharge to influence the original isotopic signals in surface water during this period. The variation in isotope composition of groundwater was less than that of surface water, and the recharge in the mountainous region was still affected in the dry season of February 2009. Furthermore, the deep aquifer, especially in a continuous and fully recharged area, exhibited a time-delay effect of precipitation (Fig. 5) and varied less in hydrochemical characters than the shallow aquifer. Generally, the isotopic compositions of hydrogen and oxygen became lighter after rainfall and became heavier due to evaporation. The heaviest measured oxygen isotope composition occurred in May 2008 and during the dry season from November 2008 to April 2009 in the pond group where the strongest evaporation was expected.

In addition, δ^{18}O in groundwater decreased after precipitation events from May to July 2008, but there was a great inconsistency in September 2008 and from March to April 2009. The presence of samples with similar time-delay effects indicated that evaporation and recharge influenced isotopic features, and further reveals the pathway and origin of the water bodies. The isotope characteristics not only reflected the local meteorological variation, plus hydrological and geochemical characteristics of groundwater, but also provided important and valuable data for the future study of landslides.

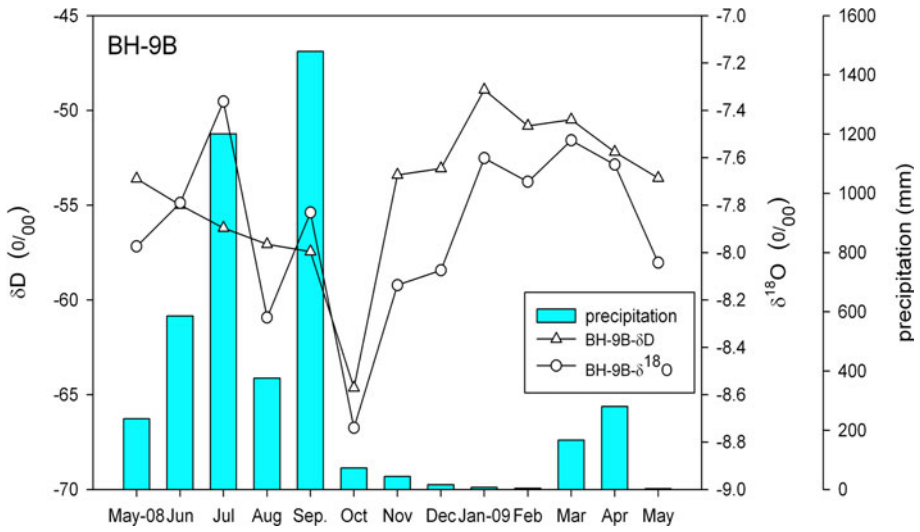

Fig. 5 Time-delay effect of 1-month on BH-9B and the monthly accumulated precipitation during the study period in the Hungtsaiping area

Spatial analysis

Integrating the study background, regional geological conditions, hydrogeochemical characteristics, and spatial distribution can help us to understand the hydrological processes in the Hungtsaiping area. Flow pathways of infiltration can be divided into unsaturated and saturated zones by using the ratio between the concentrations of sulfate and bicarbonate (Guglielmi et al. 2000). Piper diagrams were plotted to categorize the chemical types of each sample. The analytical results indicated that calcium and magnesium bicarbonate-rich water was found on the top and the middle part of the slope. In addition, sodium bicarbonate-rich water and exceptionally high sulfate concentrations were found on the foot of the slope; the sulfate content decreased with increasing elevation along the slope (Fig. 6). These conditions were excepted in BH-3B, BH-9A, BH-12A, which were acquired more deeply in the reservoir, and BH-10A, which was diluted with meteoric water from (II) Na^+–HCO_3^- into (I) Ca^{2+}/Mg^{2+}–HCO_3^- in September and December 2008.

The concentration of sulfate can be utilized to predict the possibility of landslide movement. Na^+, Mg^{2+}, Ca^{2+}, and SO_4^{2-} were chosen to analyze as predictive tools. In the top of the slope, there were low ionic concentrations except those from Moon Peach Lake, which had elevated

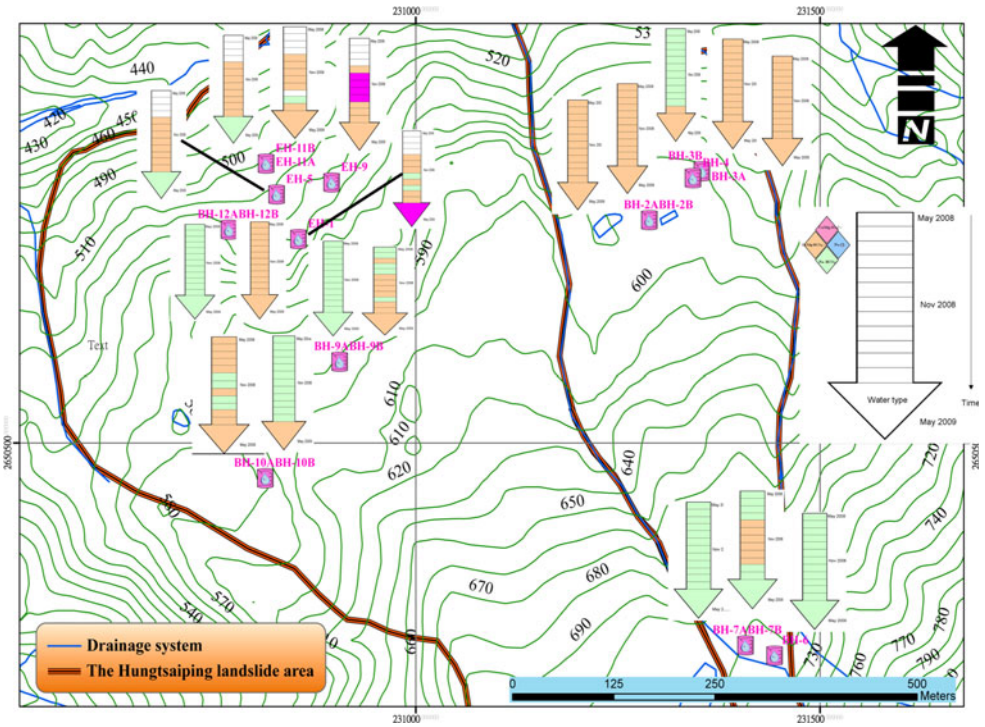

Fig. 6 The spatial and temporal variation in groundwater water types in Hungtsaiping

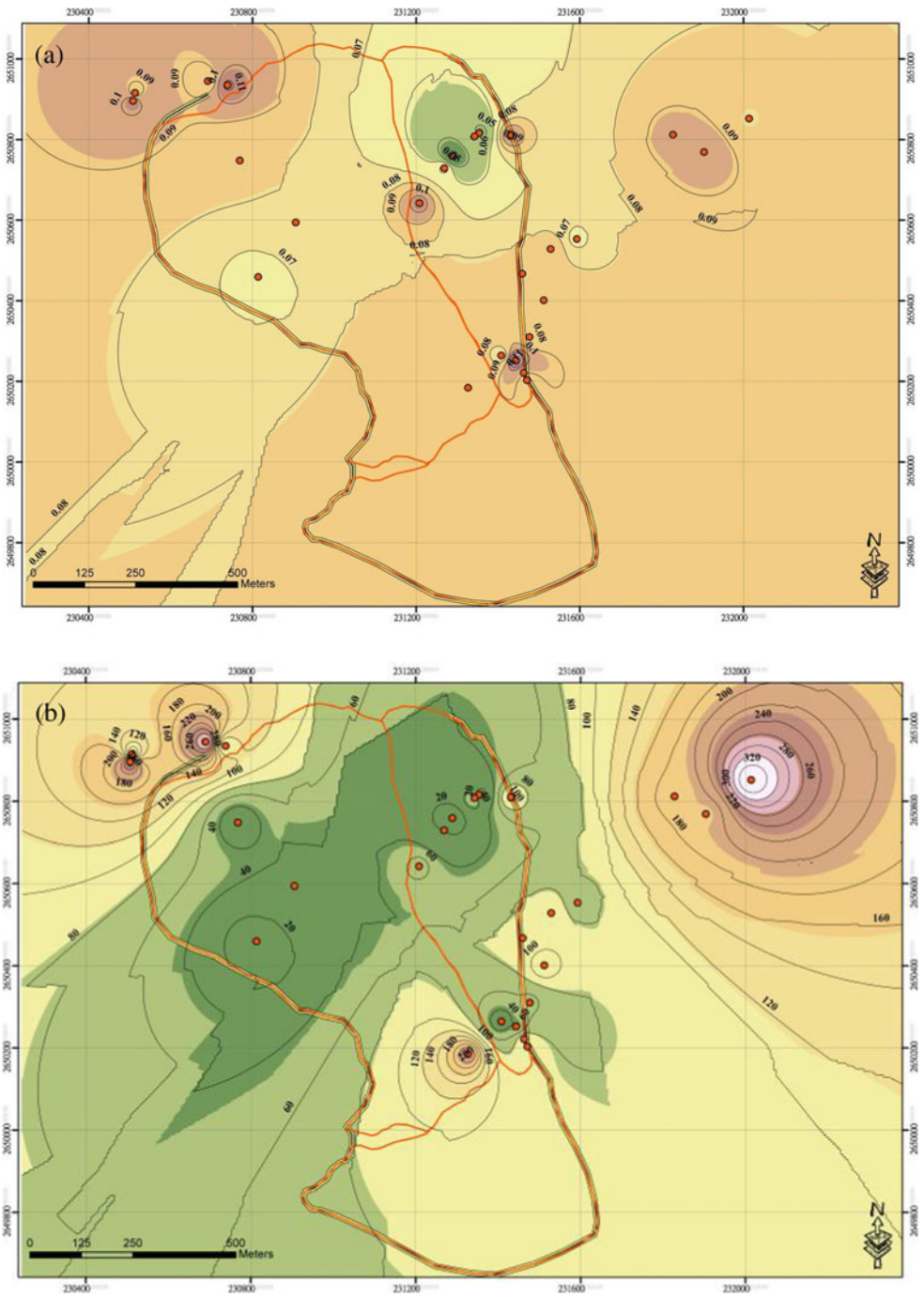

Fig. 7 Isogram: the concentration of **a** Fe^{2+}, **b** SO_4^{2-} in May 2008 in Hungtsaiping area

concentrations of Na^+ and SO_4^{2-}. Finally, the hydrogeochemical features of the slope and field investigation can be used to establish the index species for a landslide. A sampling location with high concentrations of Fe^{2+} and/or Cu^{2+} had strong oxidation–reduction reactions occurring nearby. Based on the concentration of Fe^{2+} in May 2008 from the Hungtsaiping area (Fig. 7a), the neigh-boring regions of BH-2B, BH-3A, BH-7B, BH-9A, BH-10A, BH-12A, BH-6, EH-1, EH-5, EH-11B, A Gully East-1, A Gully East-5, Moon Peach Lake, A Shao Shui Ku, Out 2-Moon Peach Alley Bridge, the Yonglu stream-1, the Yonglu stream-2 (seepages), the Yonglu stream-3 (seepages), the Yonglu stream-6 (seepages), A Gully-bottom and AB Gully-bottom had more geochemical reactions and recharge. Thus far, the hydrogeochemical data and the field observations both appear to support that the concentration of sulfate can be an index in landslide studies. For example, the concentration of sulfate in May 2008 in Hungtsaiping

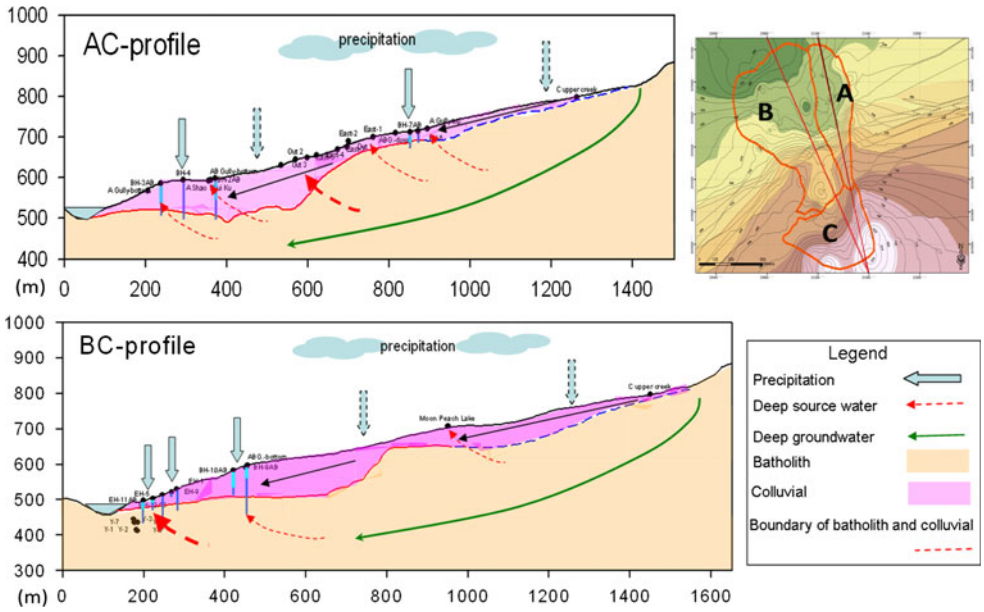

Fig. 8 The conceptual flow model of the AC and BC-profile in the Hungtsaiping landslide area

area, sulfate was enriched near the Yonglu stream, Out 1–3 and Moon Peach Lake (Fig. 7b). Moon Peach Lake was affected by man-made interference and the other locations were on unstable regions where shallow landslides occurred after heavy precipitation in the summer of 2008.

Temporal analysis

The temporal variance in the effect of precipitation on isotope composition was greater in surface water than in groundwater. The isotopic composition became lighter after a rainfall. The data were grouped in two clusters from July to October 2008. However, some samples of groundwater were lighter than surface water, which indicated that the recharge sources and conditions of the following locations were different from others: BH-2B, BH-7B, BH-4, BH-6, EH-1 and EH-11A. Comparison of these results with the time-delay effects and the isograms of the oxygen isotope composition can be utilized to determine the flow processes in the Hungtsaiping area.

Using the data of water table, precipitation, and long-term variation in the chemical species, the conditions of subsurface water infiltration can be understood. Several results were categorized by variation in their hydrochemical characteristics and water table conditions as follows: (a) the major recharge source was precipitation: BH-7A, BH-7B, BH-9B, BH-10A, BH-12B, EH-1, EH-9, EH-11A, and EH-11B; (b) the major recharge was from another stable source, not precipitation: BH-2A, BH-2B, BH-3A, BH-3B, BH-9A, and BH-10B; and (c) the recharge source was temporary and unsteady: BH-12A.

The spatial and temporal characteristics varied in terms of surface water, deep aquifers and shallow aquifers. The transmission of each water body and the sources of recharge were divided into two groups: (1) precipitation and (2) some other stable sources. The most noteworthy signals appeared around BH-7, BH-3 and EH-11; therefore, the conceptual flow model was thus established on the profiles in the Hungtsaiping landslide area.

Established profile of the Hungtsaiping area

The thickness of colluvium at each borehole, the altitude of the boundary, and the 3D Analyst-Inverse Distance Weighted of Arc-GIS were integrated in the Hungtsaiping area. Moreover, the A, B, and C zonation was combined, which was defined by Lo et al. (2008), and the profiles were sliced through the zonation of AC and BC. Projection of a shadow of the sampling locations on the AC and BC profiles can provide the distribution of the batholith and colluvium. The summarized features of the hydrogeochemical analyses can be used to create a conceptual model of the flow processes and water origin in the Hungtsaiping landslide (Fig. 8).

BH-10A was noteworthy due to its transition in type from (II) Na-HCO_3^- into (I) Ca/Mg-HCO_3^-, which was probably caused by the dilution of meteoric water from May to September 2008 and from March to May 2009. EH-9 and EH-1 responded to the type (III) Ca^{2+}/Mg^{2+}–SO_4^{2-} in a different time and space (October 2008 to January 2009 and May 2009, respectively). The extra recharge sources in a specific location and the duration of rainfall probably contributed more to the induction of a landslide.

Samples with similar time-delay effects were connected to the pathway and origin of their water bodies. The time-delay effect was more conspicuous in locations with a

longer pathway from the water body origin or with deeper recharge sources. In addition, the degree of mineralization (Na^+ and SO_4^{2-}) was high and the source was deeper in the reservoir. The concentrations of sulfate and bicarbonate can be used to differentiate between the pathways of infiltration for unsaturated and saturated reservoirs. Moreover, long-term variation in the chemical species in each groundwater sampling location can be used to define the conditions of subsurface water infiltration as follows: (a) the major recharge source was precipitation, (b) the major recharge was from another stable source, not precipitation, and (c) the recharge source was temporary and unsteady. The locations with recharge from precipitation need to be noted during the wet season. The areas with major recharge from another stable source, not precipitation, exhibited a higher probability of landslide. The geochemical characteristics can be used to represent the aquatic conditions, including the recharge conditions, flow processes, the pathway, and water origins in the slope region. Furthermore, they can be used to demonstrate the role of water in triggering landslides and can provide information useful for landslide prevention and mitigation.

Conclusions

1. Hydrochemical data revealed that the source of creeks and spring waters in the Hungtsaiping area were identical, and differed from that of ponds. Meteoric water stored in the mountain region provides recharge during the dry season. The Piper diagram showed most of the water samples belonged to type (III) Ca^{2+}/Mg^{2+}–SO_4^{2-}, where geochemical reactions were expected.
2. The local meteoric water line of the Hungtsaiping area ($\delta D = 8.4 \times \delta^{18}O + 18.0$) can be used as an isotope background in the study area. Because the recharged water in the mountainous region was still effective during the dry season of February 2009, the hydrochemical and isotopic variation of groundwater were less than those of surface water. Groundwater from the deep aquifer also exhibited a time-delayed effect of precipitation, and the results can draw a conclusion on a conceptual model of flow processes, the major recharge source and water origin in the specific landslide area.
3. Water circulation that approached the basement was more mineralized, as demonstrated by increased sulfate concentrations. Analytical results indicated that calcium and magnesium bicarbonate-rich water was found on the top and middle part of the slope, as well as sodium bicarbonate-rich water with exceptionally high sulfate concentrations, which decreased with increased elevation. Thermodynamic calculations found that the water has more sulfate concentration when it stayed in the longer route and time inside the slope; this phenomenon can be regarded as a potentially triggering factor for landslides.
4. The spatial and temporal evolutions of water can readily be explained by the analyzed hydrochemical characteristics, and then related to the landslide in the Hungtsaiping area. It is difficult to estimate the groundwater flow line in the slope region at this point, particularly because the boreholes were distributed non-linearly around the study area. However, the hydrogeochemical data in this study can still serve as a basis for prevention of landslide hazard in the future.

Acknowledgments The authors would like to thank anonymous reviewers for their constructive comments. Moreover, the authors are deeply grateful to Dr. Wang, C.H. of Institute of Earth Science, Academia Sinica; Dr. Dong, J.J. of Institute of Applied Geology, National Central University; Dr. Wang, S.L. of Department of Soil and Environmental Sciences, National Chung Hsing University; and Mr. Lee, W.R. for their guidance and support throughout this project.

Reference

Bogaard T, Guglielmi Y, Marc V, Emblanch C, Bertrand C, Mudry J (2007) Hydrogeochemistry in landslide research: a review. Bull Soc Geol Fr 2:113–126

Cappa F, Guglielmia Y, Soukatchoff VM, Mudry J, Bertrand C, Charmoille A (2004) Hydromechanical modelling of a large moving rock slope inferred from slope levelling coupled to spring long-term hydrochemical monitoring: example of the La Clapie‘re landslide (Southern Alps, France). J Hydrol 291:67–90

Chen CY, Chen TC, Yu FC, Lin SC (2005) Analysis of time-varying rainfall infiltration induced landslide. Environ Geol 48:466–479

Coleman ML, Shepherd TJ, Durham JJ, Rouse JE, Moore GR (1982) Reduction of water with zinc for hydrogen isotope analysis. Anal Chem 54:993–995

de Montety V, Marc V, Emblanch C, Malet JP, Bertrand C, Maquaire O, Bogaard TA (2007) Identifying the origin of groundwater and flow processes in complex landslides affecting black marls: insights from a hydrochemical survey. Earth Surf Process Landf 32:32–48

Epstein S, Mayeda T (1953) Variation of O-18 content of waters from natural sources. Geochim Cosmochim Acta 4:213–224

Guglielmi Y, Bertrand C, Compagon F, Follacci JP, Mudry J (2000) Acquisition of water chemistry in a mobile fissured basement massif: its role in the hydrogeological knowledge of the La Clapiere landslide (Mercantour massif, Southern Alps, France). J Hydrol 229:138–148

Guglielmi Y, Vengeon JM, Bertrand C, Mudry J, Follacci JP, Giraud A (2002) Hydrogeochemistry: an investigation tool to evaluate infiltration into large moving rock masses (case study of La Clapie‘re and Se′chilienne alpine landslides). Bull Eng Geol Environ 61:311–324

Hays WW (1981) Facing geologic and hydrologic hazards-earth science considerations. U.S. Geological Survey Professional Paper 1240(B), p 108

Huang CS, Shea KS, Chen MM (2000) Explanatory text of the geological map of Taiwan-Puli sheet. Central Geological Survey, Taiwan

Liu CN, Huang HF, Dong JJ (2008) Impacts of September 21, 1999 Chi-Chi earthquake on the characteristics of gully-type debris flows in central Taiwan. Nat Hazards. doi:10.1007/s11069-008-9223-9

Lo CM, Lin ML, Lee WC, Lee KC, Chien SY (2008) Landslide characterization and zonation of Hungtsaiping area based on topography, aerial photograph and PIV technology. Geotechnical and Geophysical Site Characterization, pp 467–472

Peng TR, Wang CH, Liu TS, Houng YL (2002) Environmental and hydrological implications revealed by hydrogen and oxygen isotope compositions for the watershed of the Wuchi system in the Nantou area. J Agric Food Chem 40:238–253

Peng TR, Wang CH, Lai TC, Ho FS (2007) Using hydrogen, oxygen, and tritium isotopes to identify the hydrological factors contributing to landslides in a mountainous area, central Taiwan. Environ Geol 52:617–1629

Peng WF, Wang CL, Chen ST, Lee ST (2008) A seismic landslide hazard analysis with topographic effect, a case study in the 99 Peaks region, Central Taiwan. Environ Geol. doi:10.1007/s00254-008-1323-z

Wang CH, Kuo1 CH, Peng TR, Chen WF, Liu TK, Chiang CJ, Liu WC, Hung JJ (2001) Isotope characteristics of Taiwan groundwaters. West Pacific Earth Sci 1:415–428

Wang WN, Wu HL, Nakamura H, Wu SC, Ouyang S, Yu MF (2003) Mass movements caused by recent tectonic activity: the 1999 Chi-chi earthquake in central Taiwan. The Island arc 12:325–334

Wei CY, Lee JF (2006) The application of digital aerial photography in the study of Hungtsaiping landslide, Chungliao, Nantou County. Bull Central Geol Surv Taiwan 19:39–59